# Structure and age relationship of joint sets on the Lilstock Benches, UK, based on mapping a full resolution UAV-based image

**Martijn A. Passchier*[1], Janos L. Urai[1], Cees W. Passchier[2]**

[1] Tectonics and Geodynamics, RWTH Aachen University, Lochnerstrasse 4-20, D-52056 Aachen, Germany, www.ged.rwth-aachen.de; URAI – ORCID 0000-0001-5299-6979

[2]Tektonophysik, Johannes Gutenberg University of Mainz, D-55099 Mainz, Germany. ORCID 0000-0002-3685-7255

*corresponding author: martijn.passchier@yahoo.de

**Keywords**: joint, Lilstock, abutment, UAV, fracturing

**Highlights**

- Full-resolution UAV-based image of the joint set of the famous Lilstock benches (UK)
- Joints are fully imaged over the whole large outcrop
- Up to eight generations of joints in a single limestone layer
- Jointing is laterally heterogeneous in the same layer
- Phases of cementation accompanied the evolution of older joints at Lilstock

## Abstract

Outcrop studies of fracture networks are important to understand such networks in the subsurface, but complete maps of all fractures in large outcrops are rare due to limitations of outcrop and image resolution. We present the first full-resolution UAV-based, Gigapixel dataset and DEM of the wave-cut Lilstock Benches in the southern Bristol Channel basin, a classic outcrop of layer-bound fracture networks in limestones. With this dataset, we mapped the patterns and age relationships of successive generations of joints in dm-thick limestone layers separated by claystone beds. Using well-defined interpretation criteria based on crosscutting relationships and joint length, up to eight generations of joints were mapped. Results show that joint geometry and interrelations are fully resolved in the whole outcrop. Different joint generations have unique characteristics in terms of shape, orientation, spatial distribution and cross-cutting relations. The presence of low-angle crossings and junctions of joints suggest periods of partial joint cementation and reactivation. The dataset and interpretations are proposed as a benchmark of a large scale, complete fracture network to test digital fracture network models.

# 1. Introduction

Joints in layered sedimentary rocks are amongst the most common and most intensely studied structures, present in nearly every outcrop. Fracture networks form important reservoirs and pathways for mineralizing fluids, hydrocarbons and water in sedimentary basins, and their density, spacing, orientation and interrelation has therefore been a subject of study since the dawn of structural geology. To model fluid flow in fractured reservoirs, the 3D network of joints must be predicted in volumes of rock large enough to be representative. A classic outcrop of faults and joint networks are the Lilstock Benches in the British Channel in the UK (51°12.166' N, 003°12.014' W; Fig. 1). The Lilstock Benches are part of the Lilstock anticline, a large intertidal outcrop of sub-horizontal layers of thin-bedded Jurassic limestone alternating with claystone layers. The limestone layers contain a dense pattern of joints, augmented by weathering, that have been studied since 1990 (Loosveld and Franssen, 1992). Key publications discuss the relation of joints to faulting (Peacock and Sanderson, 1991), fracturing (Rawnsley et al., 1998; Gillespie et al., 2011), vein formation (Peacock, 2004) and basin inversion (Dart et al., 1995; Glen et al., 2005). The local joint pattern is complex, and formed in several generations due to overprinting generations of deformation (Dart et al., 1995). The geometry of the joints has already been extensively studied on selected parts of the outcrop (Gillespie et al., 2011; Peacock, 2004) but no attempt has been made to make a complete inventory of the complete joint network in the outcrop.

The aim of this study was to analyse the joint pattern at Lilstock using a large UAV-based image, to (i) define criteria for determining the age relationship of the joints, and (ii) map the geometry and interference history of the joint network. The image covers a 350 x 700 m area of the Lilstock Benches, with a pixel size of 7.5 mm, sufficient to resolve all joints for the first time. The image we used for joint interpretation is published separately to allow verification of our results (Weismüller et al., 2020); the shapefiles shown in our figures are attached to this paper. This paper is part of three publications using the dataset (Weismüller et al., 2020).

## *1.1 Lilstock outcrop - geology*

The Bristol Channel Basin (West Somerset, UK), has experienced three main stages of deformation (Dart et al., 1995). A first stage created east-west striking normal faults, followed by north-south directed compression with partial inversion of the normal faults and folding. A third stage is NS compression, resulting in NE-SW striking sinistral strike-slip faults. Extension is thought to be lower Jurassic and Cretaceous in age, while subsequent inversion and strike-slip deformation are interpreted to be Tertiary (Dart et al., 1995; Glen et al., 2005). Burial was to a depth of about 1.5 km.

The outcrops around Lilstock present weakly deformed (Jurassic - blue Lias) sediments with large scale, open folding, faults, veins and joints formed during burial and uplift (Fig. 2B). Dm-scale limestone layers alternate with claystone beds of more variable thickness, between 4 - 71cm. The thickness of the limestone and claystone layers is laterally consistent. A single asymmetric E-W trending open anticline (Fig. 1) affects the entire outcrop with the hinge zone located directly south of the main fault. The southern limb of the fold rapidly steepens to the south while the northern limb of the anticline is less steep and outlines platforms of single exposed horizontal layers known as “benches” (Fig. 1). The anticline is attributed to the second regional deformation phase of north-south compression (Dart et al., 1995).

### *1.2 previous work on joints in Lilstock*

Papers on the joints in Lilstock usually treat small areas of this large outcrop. Some of the earliest work was by Loosveld and Franssen (1992) who used a helicopter to photograph part of the outcrop and identified up to six sets of joints. This was followed by Rawnsley et al. (1998), who identified the well-known fans of first-generation joints converging on asperities on faults. Engelder and Peacock (2001) and Belayneh and Cosgrove (2004) interpreted five to six generations of joints, describing their geometry and evolution. Figure 1 shows the approximate location of these studies, compared with the area covered in this paper. Peacock (2001) showed that there is a temporal relation between joints and faults and veins in the Lilstock outcrop (Peacock, 2004). Veins in Lilstock limestones have been studied by Caputo and Hancock (1999) and Cosgrove (2001) while faults were subject in numerous publications as well. This includes strike-slip faults (Peacock and Sanderson, 1995; Willemse et al., 1997; Kelly et al., 1998), normal faults (Davison, 1995; Nemrok and Gayer, 1996), their association with relays (Peacock and Sanderson, 1991, 1994) and normal fault inversion (Brooks et al., 1988; Chadwick, 1993; Dart et al., 1995; Nemčok et al., 1995; Kelly et al., 1999). Stress models inferred from the surface morphology of joints or aerial photographs have been studied by Belayneh (2004) and Gillespie et al. (2011). Belayneh (2003) and Belayneh et al. (2006) performed fluid injection simulation studies on the fracture network.

## 2. Materials and Methods

### *2.1 Drone data acquisition*

The entire Lilstock outcrop was photographed at low tide on 19 - 20 June 2017. Since high tide covers the outcrop, we started one day after neaps with a tidal range of 2.69m to 9.69m. The outcrop was surveyed on foot after data acquisition by drone to select key points for measurements and make detailed photographs. The drone used was a Phantom 4 model by SZ DJI Technology Co., Ltd with a 12.4-megapixel camera. Joints were photographed from an altitude of 20 – 25 m to obtain sufficient resolution to see all joints present. Photos were merged into high-resolution digital images using PhotoScan by Agisoft. The images have a pixel size of 7.5 ± 1 mm (Fig. 2C). Ground truthing was done against sub-mm resolution photographs of selected locations on the surface to validate our identification of all joints which are enhanced in visibility by wave erosion. Details on the method used, and the original dataset are published in Weismüller et al. (2020).

### *2.2 Joint mapping criteria*

We decided to map one complete Bench, part of layer IV in the local stratigraphy, to test to what extent the sequence of joints can be analysed in a completely exposed layer, and if this sequence is laterally consistent

(Fig. 1). The exposed surface of this layer (named “Bench IV”) was naturally separated into two areas (W and E) by an erosion gully. Both areas were photographed by drone and the photo mosaics mapped in detail and interpreted in terms of age relations and overall shape. Images were manually interpreted using ArcGIS. Joints were traced as polygons over their complete length. Joints were mapped and subdivided into generations using the following set of criteria:

(1) Joints that are straight or slightly curved but continuous despite crossing other joints, are interpreted as one joint, of one generation.
(2) Mapped joints are hierarchically assigned to specific generations in relation to other joints by analysis of the intersections between joints. These intersections can either be of “X” or “T” shape (abutting) (Fig. 2A). Abutting is the main argument to assign relative ages to the joints, while X-intersections do not provide such information. A secondary argument to assign joints to a specific generation is their length. In case of conflicting relations: force of number wins, provided the conflict can be explained.

Attributes such as length and orientation were extracted from ArcGIS and plotted to illustrate basic statistics. Because of time constraints, approximately every second joint was mapped to produce a representative sample and the youngest generation was only mapped in one sub-area.

# 3. Results

## *3.1 Joint imaging*

The Lilstock outcrop is extraordinary, both in the number and density of exposed joints, and in the nature of their weathering. Because of the local high tides, joints weather at the surface to a U-shape that allows imaging them with the resolution of our images (Fig. 2B-E). This weathering pattern is observed for joints in every direction while depth depends on the time period of exposure. Freshly exposed limestone layers show little weathering, although joints are still visible on our images.

## *3.2 Joints - Results of digital outcrop interpretation*

### *3.2.1 Area W*

The Western Area (Area W) of Bench IV (Fig. 1, S1) contains eight generations of joints, some of which are only present in part of this area (Fig. 3). In the western part of Area W, four generations of joints were recognized (Fig. 4C, Table 1). The first generation (J1) has the longest joints that cross the entire Area W with a NW-SE trend and even continue into layers II and III to the north (Fig. 3). In the westernmost part of Area W, the joints are abutted by a second generation, J2, (Fig. 4A) at a low angle to J1. J2-joints are mostly straight, but bend close to their termination against J1-joints, to end in a T-shaped abutting (Fig. 4A). Some J2-joints impinge upon other J2-joints.

The angle between J1- and J2-joints decreases eastwards by a change in orientation of the J1-joints, while J2 retains its orientation, till both sets of joints are subparallel. In the centre of Area W, J1- and J2-joints can no longer be distinguished, and are all mapped as J1-joints. Both generations of joints disappear towards the east (Fig. 3).

NE-SW trending J3-joints are common and closely spaced although their density can vary (Fig. 4C). J4-joints make a small angle with J3-joints. Both J3- and J4-sets are present throughout Area W (Fig. 3, 4D). Three younger generations of joints, J5 - J7, occur exclusively in the eastern part of Area W. J5-joints are subparallel to J4-joints of this area (Table 1) but locally impinge on J4-joints with a T-junction, proving their relative age. J4-joints can be further distinguished from J5-joints by their shorter length, which is consistent through Area W, and their perfectly straight geometry. J5-joints tend to be slightly curved (Fig. 4D).

J6-joints are strongly curved in contrast to all older generations. They impinge on J4- and J5-joints with a T-junction confirming their relative age. J7-joints trend approximately N-S and abut all previous generations in T-shapes in locations where J5-joints and J6-joints intersect (Figs. 3, 4D).

The youngest joints (J8) have variable orientation, abutting against all older joints and never crossing them (Fig. 4F, S2). The density of J8-joints varies between stratigraphic layers of different thickness, creating different sized limestone blocks. However, block size also depends on the density of older generation joints. Stratigraphic layer IV is twice as thick as layer III (Fig. 1), but the limestone blocks delimited by J8-joints in Bench IV are smaller than in the adjacent layer, while the opposite would be expected. This could be due to the density of older joints that is much higher in layer IV than in the stratigraphic layers above, creating smaller blocks.

### *3.2.2 Area E*

The eastern part of the investigated Bench IV, Area E, comprises a large exposed bench of the same layer IV as in Area W, and separated from it by a gully and a domain where joint generation cannot easily be attributed. (Fig. 5, Table 1). Labelling in this part of the bench follows that of Area W, where more generations are present, with addition of an asterisk. Joints recognised in Area E are J1*, J4*, J5*, J6* and J8*.

J1*-joints show pronounced fanning, converging on a fault (Gillespie et al. 2011) and thin out towards the centre of the area. The same relation can be found, with smaller fans, in other stratigraphic layers, always related to the main fault. Single J1*-joints cross most of the Bench in a SE-NW direction. Shorter joints can be observed to abut joints of the same generation, continuing in the same direction. Two smaller fans of J1*-joints are visible on Bench IV as well (Fig. 5). In the western most part of Area E, the J1*-joints have a trend of 140-150° and are shown to be older than J4*.

J4*-joints strike in the same direction and show the same characteristics as J4-joints of Area W, being the only example of joints that are easy to correlate over the entire Bench IV. J4* occurs throughout Area E, while other generations occur in a patchy manner.

J5*- and J6*-joints are spatially separated, with only a small area of overlap where they show their relative age through abutting (Fig. 5). J5* is restricted to the western part of Area E but seem to cross into stratigraphic layer III north of Area E. J6*- and J4*-joints abut each other in T-intersections with equal frequency (Fig. 6A). This would seem to contradict the described method of age determination through T-intersections. However, since J4*-joints are clearly and consistently abutted by J5*-joints, and these J5*-joints in turn are abutted by J6*-joints, the age relation can be indirectly determined (Fig. 6B). The youngest generation (J8*) in Area E is similar to J8 in Area W, occurring perpendicular to older joints. However, in Area E there are domains of approximately 10x10 m with only a few J4* and many J8* joints resulting in joint networks made up of nearly only J8*.

The transitional domain of Bench IV between areas W and E contains numerous joints in various directions, but impingement relations are not clear since older joints cannot be followed for a long distance in the narrow Bench (Fig. 1). The reason is probably that joints of different generations happen to lie at a small angle with each other, and older joints may have been reactivated to impinge on younger joints. This makes age relations unclear. In Areas W and E, intermediate generations of joints occur which allow distinction of joint generations.

Outside Bench IV, joint generation sequences and orientation may deviate from those in Bench IV, but relations have not yet been mapped. For example, in layers south of Area W, the locally oldest generation of joints follows the same orientation as the hinge line of the main fold. This parallelism to the foliation of the fold appears over a large area and across multiple stratigraphic layers. Different stratigraphic layers seem to have different sets of joints. While most layers have 2-3 generations, Bench IV shows up to 8 generations of joints with a maximum of approximately four generations being present on a 10m scale surfaces.

# 4. Discussion

This study presents a manually interpreted map of joints in the famous Lilstock Benches, based on a complete digital image of the outcrop. Previous work has either used stitched photos of parts of the outcrop, or images without the resolution to resolve all joints. Preparing the image was possible because the joints are augmented by wave erosion, which allowed imaging all joints in this large outcrop with a UAV in one single day. Comparison with close-up photos (with much higher resolution) of selected sites validates that the resolution chosen is indeed sufficient: all joints are visible on our image (Weismüller et al., 2020). Our observations are generally in agreement with existing studies, which have shown that the joints are younger than the faults and veins in the outcrop, and developed during uplift, with stress concentrations at fault asperities during the development of the first joint generation, causing the well-known joint fans also present in other outcrops around the Bristol channel (Bourne and Willemse, 2001; Maerten et al., 2018).

Our study shows that it is not possible to assess the full joint generation content of the Lillstock Benches by study of a small representative area. Because of the larger extent or our database compared to earlier studies, we can give a more complete and more complex image of the structural content of one specific layer in the stratigraphy, Bench IV. First analysis of the joints sets present in Bench IV show, that at least eight generations of joints are present over the entire Bench, but that several generations are always missing in smaller parts of the outcrop (Fig. 7). In some 10x10m domains of the investigated area four generations are present, but rarely more (Figs. 4, 6).

### *4.1 Robustness of interpretation*

In agreement with earlier studies, we found that, since joints do not deform or displace older joints, mapping of joint sets and distinguishing different generations is generally possible based on a few simple criteria:

1. joints that are straight or slightly curved but continuous despite crossing other joints, are interpreted as one joint.
2. joint intersections can either be in an "X" or "T" shape. T-shaped geometries are the main argument to assign relative ages to the joints.
3. assigning joints to a specific generation is by orientation, abutment and also consistent with their length: the longest joints are generally oldest.

A number of cases where analysis based on these criteria failed are discussed below. To check the robustness of the interpretations, selected areas were mapped by a second interpreter using the same criteria, with very similar results.

In Table 1 we compare the different joint generations interpreted by previous studies with the generations found in this project, as far as possible. The locations of the studied joints of previous publications are included in Figure 1. Generations of joints presented in the literature but missing in this paper, can also be the result of these studies being done on a different bench. Although it is possible to recognise generations of joints, the nature of the structure imposes inherent problems that are outlined below.

### *4.2 Joint generations*

#### *4.2.1. The oldest joints and lack of overprint*

The oldest joints, J1 and J1* are fanning from a number of discrete points on the faults, are continuous, longer than the outcrop dimensions, and never abut against older joints (Figs. 3, 5). In the arches between the joint fans there are areas completely devoid of J1* joints. The local absence of J1/ J1*-joints could be due to a lateral change in the stress field, or lateral variations in lithology. Because of their length, continuity and absence of abutting, J1 are clearly the oldest joints present. In the west of Bench IV (Area W), J1-joints show a low angle to J2, which consistently abut against J1. Towards the east, J1 gradually changes in orientation until it is indistinguishable from J2. In our interpretation J2 joints formed late during the J1 phase, when the local minimum stress in the west of the bench rotated slightly. Although J2-joints are only known from the western part of Area W, they may be distributed throughout Bench IV as a later generation of J1-joints, which can only be recognised where they make an angle with older J1-joints. This problem is not inherent for joints; similar problems could be envisaged for the interference of different generations of folds and foliations in other areas.

#### 4.2.2. Intermediate generations

Joints of generations J3, J5/J5*, J6/J6* and J7 have a limited distribution over Bench IV (Table 1, Figs. 3-5, 7, S1), while J4/J4* occurs throughout the Bench. J3 (Fig. 4C) only occurs in the west and did not propagate elsewhere. In a similar way, J5/J5* and J6/J6* are restricted in distribution, where J5, J6 and J7 overlap in distribution in Area W, and J5* and J6* partly overlap in Area E (Fig. 4E, 7). Possibly, conditions for joint generation were similar in this part of the outcrop during propagation of these generations in terms of the local lithology and layer thickness of Bench IV. Interestingly, J5 occurs in Area W where J4 is less dense, in a very similar orientation, while J5* has a very different orientation in Area E. Possibly, there is a rotation of the stress field after development of J4 in similar manner to that of J2 after J1.

#### 4.2.3. Youngest generation joints

Joints of the youngest generation (J8/J8*) are the most numerous, in terms of total length of joints per $m^2$. They abut against older joints, and do not cross these, probably because these youngest joints formed during uplift, when older joints had opened (Fig. 4F, S2). J8/J8* joints have highly variable orientation. This indicates that these joints formed in the remaining unjointed islands until the layer was saturated, their orientation controlled by the surrounding older joints of different generations. Interestingly, Figure 6C shows an example where the recursive abutting of joints creates an "Escherian paradox" (Penrose and Penrose, 1958) where age relationships based on abutment criteria fails. We interpret this to indicate that the four joints nucleated simultaneously, and grew until abutting in the recursive set.

### 4.3 Joints in different layers

Although not discussed this in detail in this paper, joint patterns in different layers (or benches) are quite different (Fig. 3). Bench IV, where our observations were made is the thickest limestone layer present in the outcrop, and seems to have the largest number of joint generations. The oldest generation joints are present in several layers, while younger joints are absent or of different geometry in any other layers. The current explanation for this is given in an analysis by Bourne (2003) who considered the formation of a joint set in one layer of a multilayer, and its effect on the stress field and the initiation of subsequent joints in adjacent layers. Similar effects can be seen in Lilstock (Prabhakaran et al, in prep).

### 4.4 X-intersections

Joint generations in this study could be recognised because of abutment of younger joints on older ones. Abutment is characterised by a T-junction, where the younger joint does not cross over an older one, while in many cases the younger joint changes direction close to the older joint, to impinge at higher angle that the far-field orientation (Figs. 4, 6). Abutting is common when older joints are non-cemented. Bench IV, however, shows many examples of intersections where joints cross even at a small angle, so called X-intersections (Figs. 4, 6). X-junctions provide no information on age relations, but are interesting, since they provide constraints on stress conditions during joint interaction and the nature of joint sealing (Renshaw and Pollard, 1995). In our dataset, X junctions between joints can occur at a very small angle, down to 5° (Fig. 6D). In Bench IV, X-intersections are especially common for the older generations of joints, and one joint can commonly cross several older joints of even multiple generations before finally abutting on a joint of an older set. The presence of such low angle X-intersections is intriguing, because if joints are uncemented fractures, even with very high anisotropy of the horizontal stress, crosscutting is not possible at such a low angle (Renshaw and Pollard, 1995): instead, the younger joints will abut on the older one without crossing over into the adjacent block. However, joints can cross older joints if cementation of the older joint partly restores the shear strength (Virgo et al., 2013, 2014, 2016). If joints are completely invisible to the stress field because they are “glued” together with a vein of exactly the same strength and elastic modulus, joints can cross without any deflection. However, if mineralisation of joints is partial or if sectors of joints are immobilised by jogs, so that these parts remain open and fluid filled, joints may cross older ones with small deflections. In Bench IV of Lilstock, no macroscopic deflection is visible for most X-junctions, and we propose that the older joints were at least partially cemented before the younger generation crossed these. They had refractured, however before the formation of J8 and J8* joints, which always abut on older joints. Microscopic investigation of un-weathered joints in the area could show to what extent partial cementation by microveins is present.

### *4.5 Polyphase joints - reactivation*

Our observations suggest, that joints belonging to one generation may have formed in several time steps, and that some continuous joints are polyphase in nature. An example is seen for J4*-joints and J6*-joints, which impinge on each other while the joint sets are clearly separated by J5*-joints (Fig. 4E, 6A, B). Probably, some J4*-joints are reactivated and restart growing with the new segments in the same orientation, to impinge on older parts of newly formed J6*-joints. Another observation showed two- J1-joints that apparently stopped growing, and were reactivated when J2-joints formed, with the new segment following the direction of the second generation with a sharp kink (Fig. 4B). The result is a rhomb-shaped form defined by two sets of parallel J1- and J2-joints, mutually abutting. Polyphase joints can therefore be of two types: those that continue growing in the same direction, since the stress field is similarly oriented, and those that nucleate on the tip of older joints, and propagate in a new direction. Such nucleation occurs in Bench IV up to an angle of at least 17° (Fig. 4b). At larger angles the new, and in some cases, the old segments can open and form a transition to pennant veins (Coelho et al., 2006) and wing cracks (Conçalves and Einstein, 2013; Kolari, 2017).

### *4.8 Joint length and age*

Although not measured in detail, a correlation seems to exist on Bench IV between joint length and age (Figs. 3,5). In the investigated area, the oldest generations are the longest, and progressive younger generations of joints produce shorter joints (Fig. 3), although exceptions can be found: J4-joints are shorter than J5. The explanation for the decrease in length with age can simply be that, although J1-joints could propagate trough pristine, undeformed layers of rock, successively younger generations would necessarily interact with pre-existing joints, increasing the chance to meet partly cemented or open joints that could not be crossed (e.g. Fig. 6A). Although joints may transect cemented parts of some layers, they will eventually strike an uncemented part of a joint, and their length will therefore be determined by the mean distance between older joints that are crossed. Joint length is very limited for the last generation, J8/J8*, probably because these joints formed during uplift, when many cemented joints reopened, blocking joint propagation.

Certain generations, such as J3 and J4-J4* seems to have a dominant characteristic length that cannot only be explained by interaction with older joints, since they partly occur in domains where no older joints are present (Figs. 3, 4C, 4D, 5). Their characteristic length may be explained by the nature of the stress-field in Bench IV and the adjacent claystone layers, which must have been different from that during generation of the long, early joints J1/J1* and J2

# 5. Conclusions

1) The Lilstock outcrop in the Bristol channel shows evidence for eight generations of joints, up to four in each location on a 10m scale. These generations are distinguished by a fixed set of criteria, set up for this study but generally applicable.
2) Joints of one generation can terminate on older joints or cross them, creating X or T junctions
3) Joints can cross other joints at very small angles, down to 5°, without deflection. This is interpreted to mean that such older joints were mechanically inactive, and invisible in the stress field
4) Different stratigraphic layers have different sets of joints. Most layers have 2-3 and only one layer (IV), with maximum thickness, has 8 generations
5) There is a correlation between joint length and age - oldest joints are the longest
6) Crosscutting of one generation of joint by the next mostly occurs in older joints generations. The youngest generation do not commonly cross older joints, probably because these older joints are opening with uplift
7) The youngest generation of joints (J8 and J8*) has only T-junctions
8) Joint generations cannot be recognized exclusively by their orientation and cannot always be distinguished if they fan into parallelism

# Acknowledgements

Christopher Weismüller is thanked for the drone imaging and the processing of images into a GIS file and for many discussions.

# References


BELAYNEH, M. 2003. Analysis of natural fracture networks in massive and well-bedded carbonates and the impact of these networks on fluid flow in dual porosity modelling. Thesis, Imperial College London (University of London).

BELAYNEH, M. 2004. Palaeostress orientation inferred from surface morphology of joints on the southern margin of the Bristol Channel Basin, UK. Geological Society, London, Special Publications, 231, 243-255.

BELAYNEH, M. and COSGROVE, J.W. 2004. Fracture-pattern variations around a major fold and their implications regarding fracture prediction using limited data: an example from the Bristol Channel Basin. Geological Society, London, Special Publications, 231, 89-102.

BELAYNEH, M., GEIGER, S. and MATTHÄI, S.K. 2006. Numerical simulation of water injection into layered fractured carbonate reservoir analogs. AAPG Bulletin, 90, 1473-1493.

BOURNE, S. J. and WILLEMSE, E. J. M. 2001. Elastic stress control on the pattern of tensile fracturing around a small fault network at Nash Point, UK. Journal of Structural Geology 23, 1753-1770

BROOKS, M., TRAYNER, P.M. and TRIMBLE, T.J. 1988. Mesozoic reactivation of Variscan thrusting in the Bristol Channel area, UK. Journal of the Geological Society, 145, 439-444.

BOURNE, S.J. 2003. Contrast of elastic properties between rock layers as a mechanism for the initiation and orientation of tensile failure under uniform remote compression. Journal of Geophysical Research: Solid Earth, 108, p. 2395

CAPUTO, R. and HANCOCK, P.L. 1999. Crack-jump mechanism and its implications for stress cyclicity during extension fracturing. Journal of Geodynamics, 27, 45-60.

CHADWICK, R.A. 1993. Aspects of basin inversion in southern Britain. Journal of the Geological Society, London, 150, 311-322.

COELHO, S., PASSCHIER, C., MARQUES, F. 2006. Riedel-shear control on the development of pennant veins: Field example and analogue modelling. Journal of Structural Geology, 28, 1658-1669.

CONÇALVES DA SILVA, B. and EINSTEIN, H. H. 2013. Modeling of crack initiation, propagation and coalescence in rocks. International Journal of Fracture 257563978. DOI 10.1007/s10704-013-9866-8

COSGROVE, J.W. 2001. Hydraulic fracturing during the formation and deformation of a basin: a factor in the dewatering of low-permeability sediments. AAPG Bulletin, 85, 737-748.

DART, C.J., MCCLAY, K. and HOLLINGS, P.N. 1995. 3D analysis of inverted extensional fault systems, southern Bristol Channel basin. *In:* Buchanan J.G. and Buchanan P.G. Basin Inversion, (ed.), Geological Society Special, 88, 393-413.

DAVISON, I. 1995. Fault slip evolution determined from crack-seal veins in pull-aparts and their implications for general slip models. Journal of Structural Geology, 17, 1025-1034.

ENGELDER, T. and PEACOCK, D.C.P 2001. Joint development normal to regional compression during flexural-flow folding: the Lilstock buttress anticline, Somerset, England. Journal of Structural Geology, 23, 259-277.

GILLESPIE, P., MONSEN, E., MAERTEN, L., HUNT, D., THURMOND, J. and TUCK, D. 2011. Fractures in carbonates: from digital outcrops to mechanical models. Society for Sedimentary Geology, 10, 137-147.

GLEN, R.A., HANCOCK, P.L. and WHITTAKER, A. 2005. Basin inversion by distributed deformation: the southern margin of the Bristol Channel Basin, England. Journal of Structural Geology, 27, 2113-2134.

KELLY, R.G., SANDERSON, D.J. and PEACOCK, D.C.P. 1998. Linkage and evolution of conjugate strike-slip fault zones in limestones of Somerset and Northumbria. Journal of Structural Geology, 20, 1447-1493.

KELLY, P.G., PEACOCK, D.C.P, SANDERSON, D.J. and MCGURK, A.C. 1999. Selective reverse-reactivation of normal faults, deformation around reverse-reactivated faults in the Mesozoic of the Somerset coast. Journal of Structural Geology, 21, 493-509.

KOLARI, K. 2017. A complete three-dimensional continuum model of wing-crack growth in granular brittle solids. International Journal of Solids and Structures 115-116, 27-42.

LOOSVELD, R.J.H. and FRANSSEN, R.C.M.W. 1992. Extensional vs. shear fractures: implications for reservoir characterisation. Society of Petroleum Engineers, SPE 25017, 23-30. Nemčok and Gayer 1996

MAERTEN, L, MAERTEN, F, LEJRI, M. 2018. Along fault friction and fluid pressure effects on the spatial distribution of fault-related fractures Journal of Structural Geology, 108, 198-212.

NEMČOK, M., GAYER, R. and MILIORIZOS, M. 1995. Structural analysis of the inverted Bristol Channel Basin: implications for the geometry and timing of fracture porosity. *In:* Buchanan, J.G. and Buchanan, P.G., (ed.), Basin Inversion. Geological Society, London, Special Publications, 88, 355-392.

PEACOCK, D.C.P. and SANDERSON, D.J. 1991. Displacements, segment linkage and relay ramps in normal fault zones. Journal of Structural Geology, 13, 721-733.

PEACOCK, D.C.P. and SANDERSON, D.J. 1994. Geometry and development of relay ramps in normal fault systems. AAPG Bulletin, 78, 147-165.

PEACOCK, D.C.P. and SANDERSON, D.J. 1995. Strike-slip relay ramps. Journal of Structural Geology, 17, 1351-1360.

PEACOCK, D.C.P. 2001. The temporal relationship between joints and faults. Journal of Structural Geology, 23, 329-341.

PEACOCK, D.C.P. 2004. Differences between veins and joints using the example of the Jurassic limestones of Somerset. *In:* Cosgrove J.W. and Engelder T. The Initiation, Propagation, and Arrest of Joints and Other Fractures, (ed.), Geological Society, London, Special Publications, 231, 209-221.

PENROSE, L. S. and PENROSE, R. 1958. Impossible objects: a special type of visual illusion. British Journal of Psychology, 49, 31-33.

RAWNSLEY, K.D., PEACOCK, D.C.P., RIVES, T. and PETIT. J.-P. 1998. Joints in the Mesozoic sediments around the Bristol Channel Basin. Journal of Structural Geology, 20, 1641-1661.

RENSHAW, C.E. and POLLARD, D.D. 1995. An experimentally verified criterion for propagation across unbounded frictional interfaces in brittle, linear elastic materials. International Journal of Rock Mechanics and Mining Sciences and Geomechanics Abstracts, 32, 237-249.

VIRGO, S., ARNDT, M., SOBISCH, Z., URAI, J.L. 2013. Development of fault and vein networks in a carbonate sequence near Hayl al-Shaz, Oman Mountains. GeoArabia, 18, 99-136.

VIRGO, S. ABE, S. and URAI, J.L. 2014. The evolution of crack seal vein and fracture networks in an evolving stress field: Insights from Discrete Element Models of fracture sealing. Journal of Geophysical Research: Solid Earth, 119, 8708-8727.

VIRGO, S. ABE, S. and URAI, J.L. 2016. The influence of loading conditions on fracture initiation, propagation, and interaction in rocks with veins: Results from a comparative Discrete Element Method study. Journal of Geophysical Research: Solid Earth, 121, 1730-1738.

WEISMÜLLER, C., PRABHAKARAN, R., PASSCHIER, M., URAI, J.L., BERTOTTI, G. and REICHERTER, K. 2020. Mapping the fracture network in the Lilstock pavement, Bristol Channel, UK: manual versus automatic. Solid Earth Discuss., https://doi.org/10.5194/se-2020-67.

WILLEMSE, E.J.M. 1997. Segmented normal faults: Correspondence between three‐dimensional mechanical models and field data. Journal of Geophysical Research: Solid Earth, 102, 675-692.

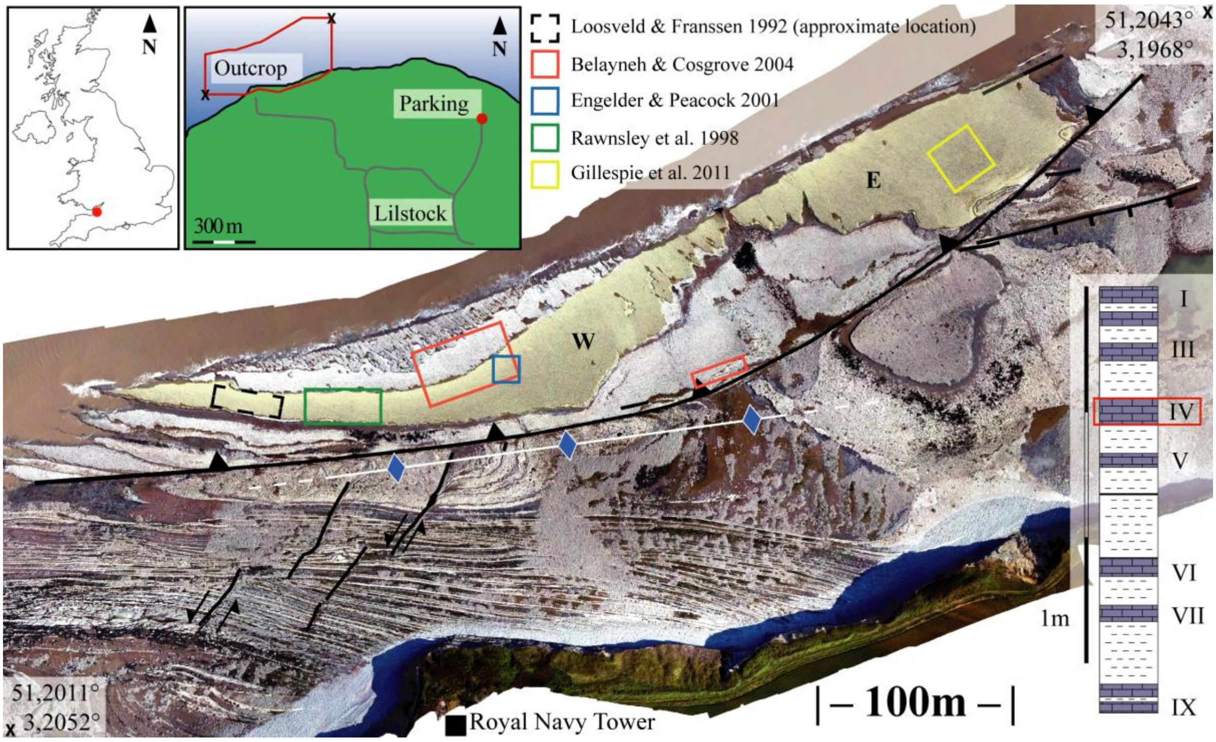


Figure 1: Overview of the main part of the Lilstock Benches in a merged digital image, taken from 100m altitude. Bench IV, an outcropping part of layer IV is highlighted in yellow, the main faults in black, the anticline in white with blue arrows. W and E – areas W and E of Bench IV. Locations of previous work on joints in the literature shown as coloured rectangles. Location of Lilstock in the UK and the outcrop at Lilstock Beach, outlined in red shown in insets at top left. The stratigraphic column of the clay and limestone benches shown at bottom right, highlighting layer IV.

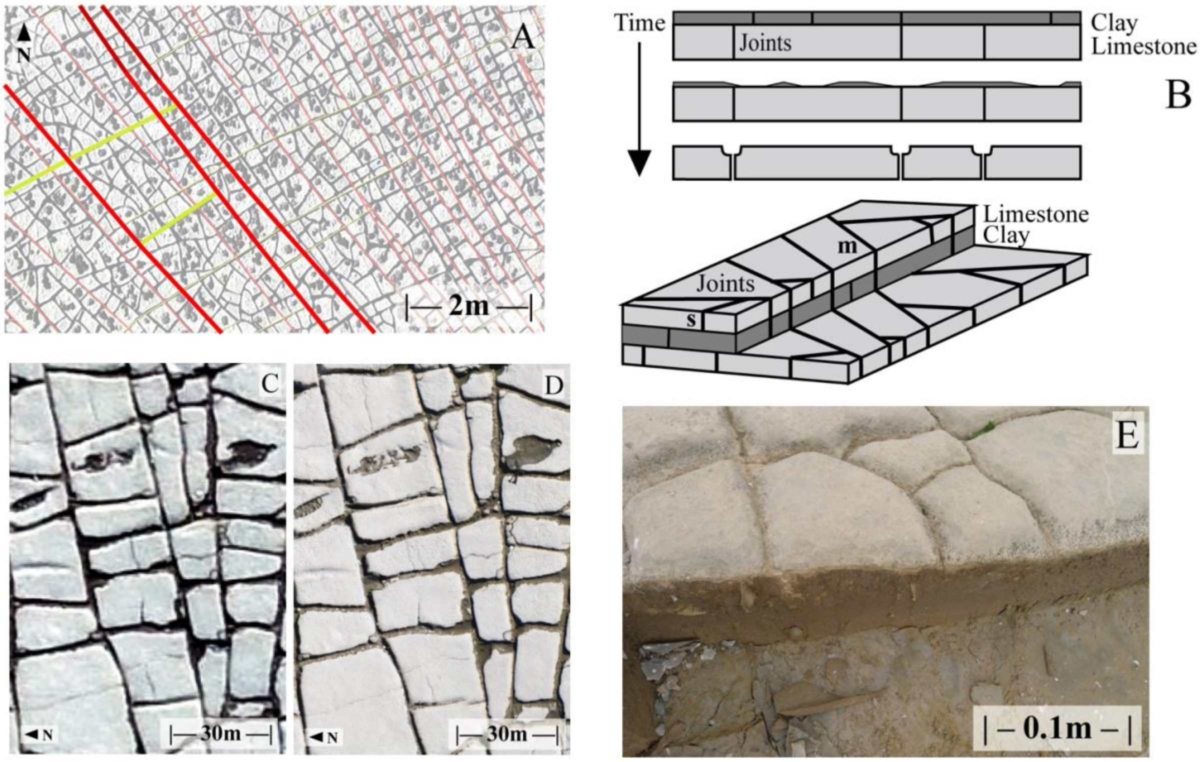


Figure 2: **A**: example of T and X intersections between J1* (red) and J4* (yellow) joints in Area E. **B**: Weathering process erodes joints to a "U" shape that makes them visible from a distance. Joint can be formed within only one layer (s) or can cross into multiple layers above and below (m). **C**: resolution used for this study of 7.4mm pixel size compared to (D) the resolution of field photography with 2.2mm pixel size .(E). field photo of typical eroded joints of Bench IV.

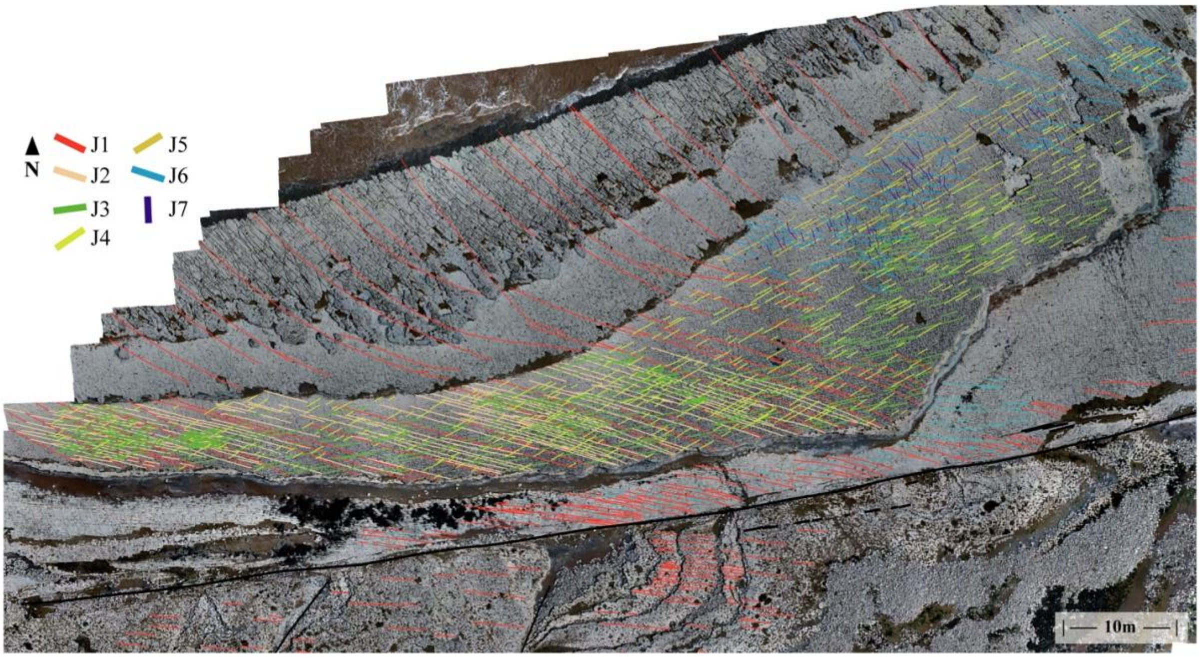


Figure 3: Overview of Area W with all mapped generations marked in colour, except for the youngest, J8. Visible are J1 and J2 approaching sub-parallelism in the centre of the layer and the local aspect of some generations.

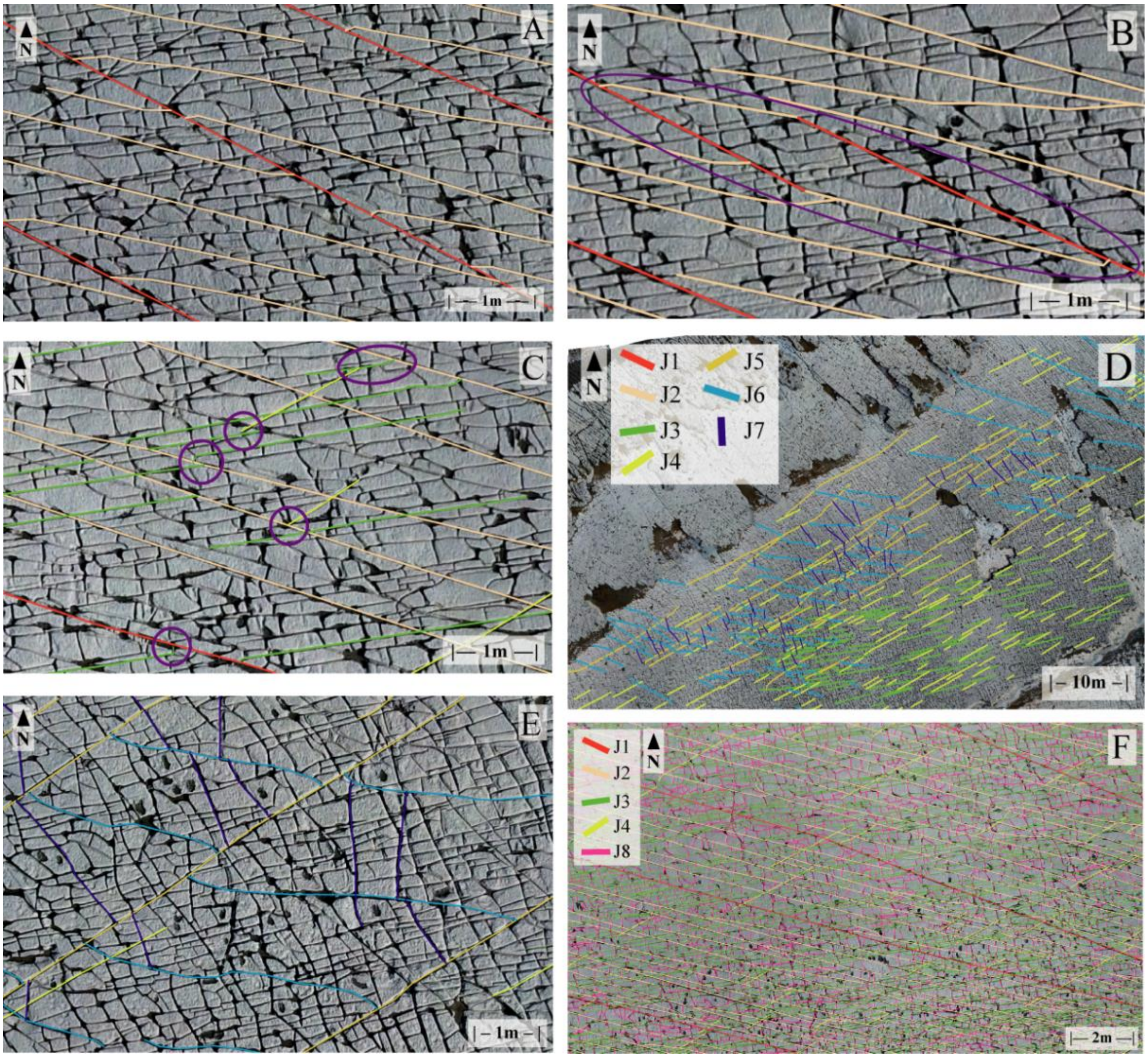


Figure 4: Interaction of different generations of joints in Area A. Selected joints have been marked in colour for clarity. (**A**) J2- joints (beige) of Area W abut on J1-joints (red). (**B**) Rhomb shaped form (marked by pink oval) between J1 and J2, caused by mutual impingement, probably due to reactivation of J1 joints during generation of J2. (**C**) Abutment relations of generations J1 (red), J2 (beige), J3 (green) and J4 (yellow) in Area W. Pink circles show abutting. (**D**) Enlarged north-eastern part of Area W with locally occurring generations: J5, J6 and J7. The more widely distributed J3 and J4 are also present, while J1 and J2 are not developed in this location. (**E**) Strongly curved J6 joints (light blue) impinging on J5 (yellow). J7 joints dark blue. Curvature is such that it increases the impingement angle. (**F**) Section of outcrop with all joints highlighted: J1-J4 and J8.

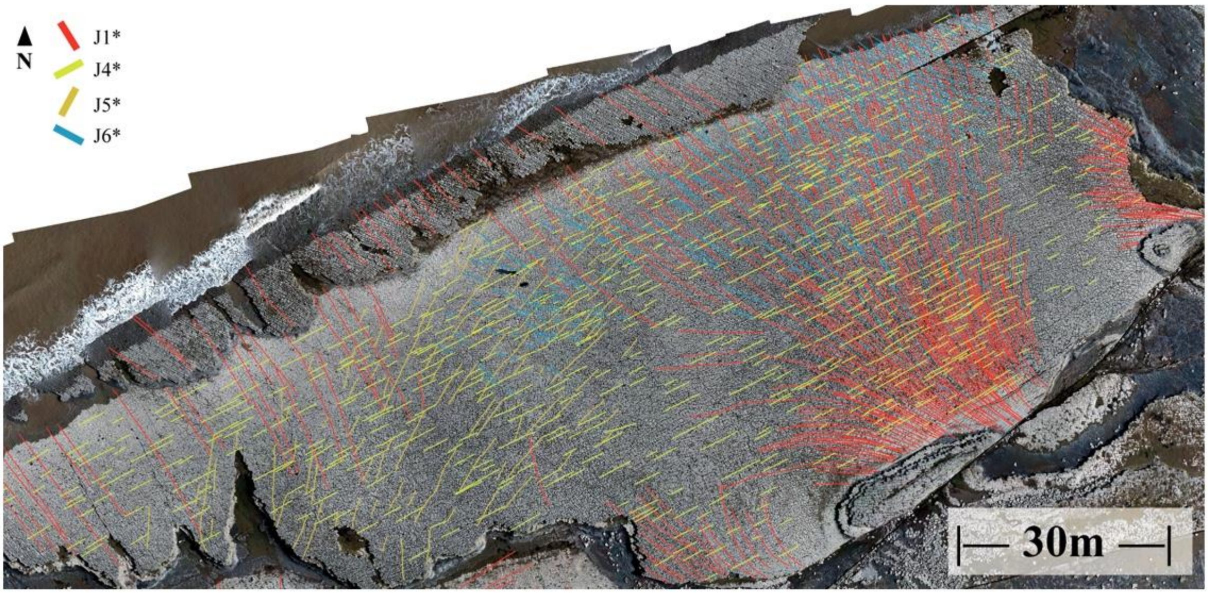


Figure 5: Overview of Area E with all mapped joint generations except the youngest J8*. J5* and J6* occur mostly in separate locations with only a small area of overlap.

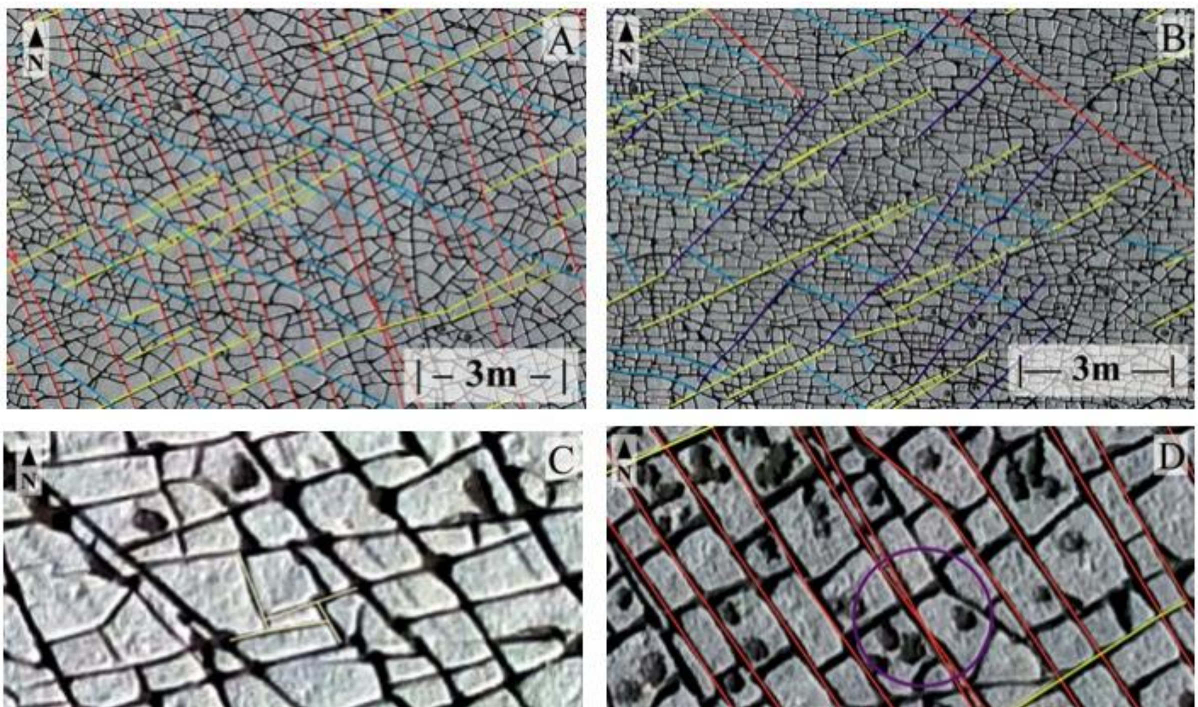


Figure 6: Interaction of different generations of joints mostly from Area B. Selected joints have been marked in colour for clarity. (**A**) Apparently conflicting abutting relations between J4* (yellow) and J6* (light blue). These generations are abutting each other equally often. (**B**) J6* clearly abut to J5*, which abuts to J4* resolving the age-relationship. (**C**) four J8-joints from Area A forming an Escherian paradox through T-intersections that contradict the simple analysis based on sequential joint growth. (**D**) The smallest angle of crossing joints could be observed between two J1* joints at 5° (marked by a circle).

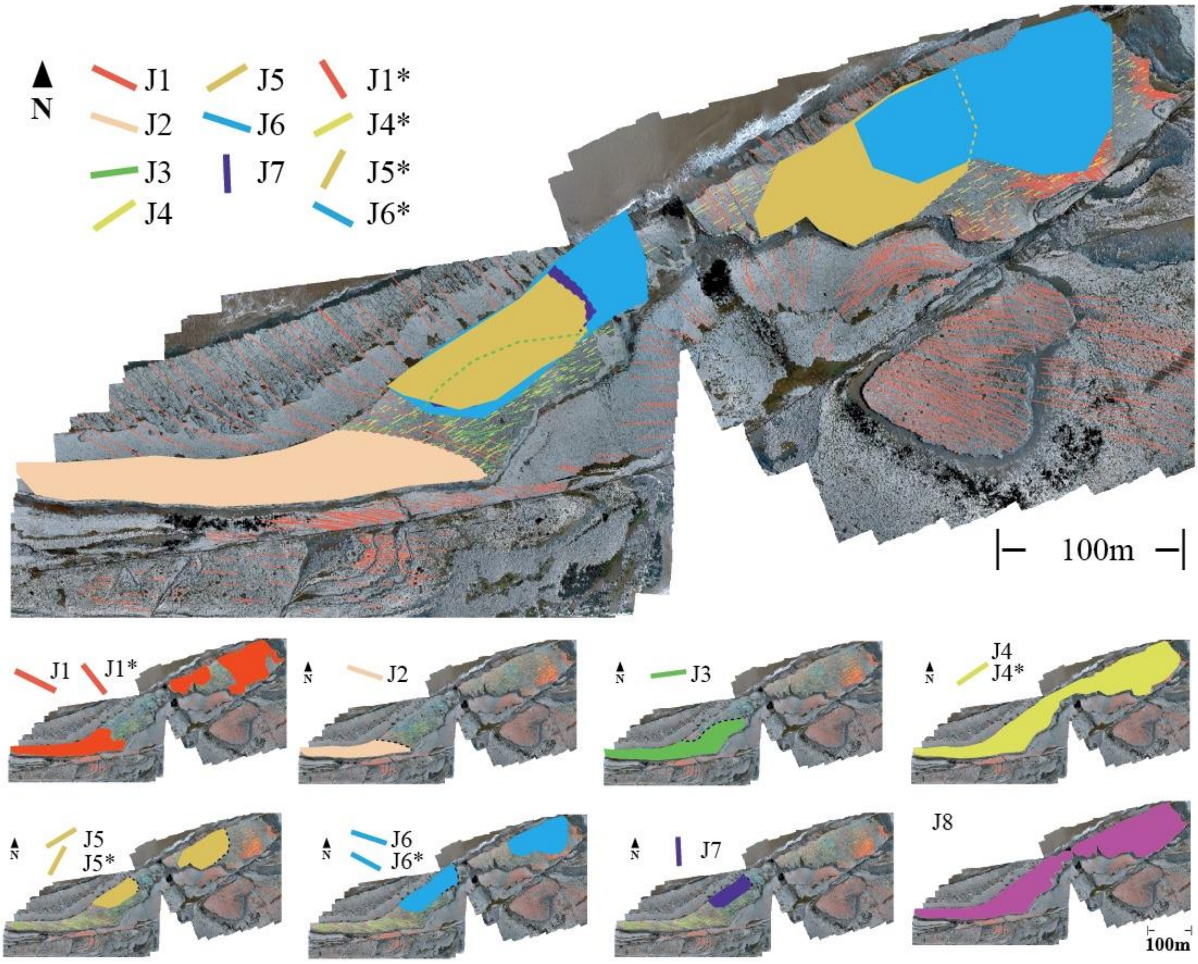


Figure 7: Distribution of all joints over Bench IV. General distribution is shown at the top, individual generations at the bottom.

| East | | West | | Generations in literature | | | |
|---|---|---|---|---|---|---|---|
| Generation<br>Angle<br>Length [m] | Curvature Properties | Generation<br>Angle<br>Length [m] | Curvature Properties | B&C | E&P | L&F | Rea |
| J1<br>115-120°<br>30-50 | straight | J1*<br>300-340°<br>10-30 | fanning out connected to fault | J1<br>115-120° | J2<br>115-120° | 1 | 3<br>125-130° |
| J2<br>100-105°<br>6-10 | straight, curve into T junction | | | J2<br>110-115° | J4<br>95-105° | 2 | 4<br>100-110° |
| J3<br>80°<br>6-15 | straight, most common | | | J3<br>85-95° | J6<br>75-85° | 3&4 | |
| J4<br>60°<br>1-4 | straight consistent | J4*<br>60-65°<br>1-6 | straight consistent | J4<br>65-70° | | 5 | |
| J5<br>55-60°<br>10-20 | lightly curved local presence | J5*<br>5-40°<br>2-5 | straight | | | | |
| J6<br>100-110°<br>4-8 | strongly curved local presence | J6*<br>110-130°<br>1-3 | slightly curved | | | | |
| J7<br>340-10°<br>2-5 | straight local presence | | | J6<br>335-345° | | | |
| J8<br>variable<br><0.5 | curvy irregular | J8*<br>variable<br><0.5 | straight | | | | |

Table 1: Joint generations and their characteristics in Areas W and E, as well as the connections that can be observed between generations in both areas. Included at the right side are joint generations described in other publications that can be related to here identified generations. Non assignable generations are omitted, angles are given if provided in the literature. B&C - Belayneh and Cosgrove (2004); E&P - Engelder and Peacock (2001); L&F - Loosveld and Franssen (1992); Rea - Rawnsley et al. (1998).

# Supplementary Figures

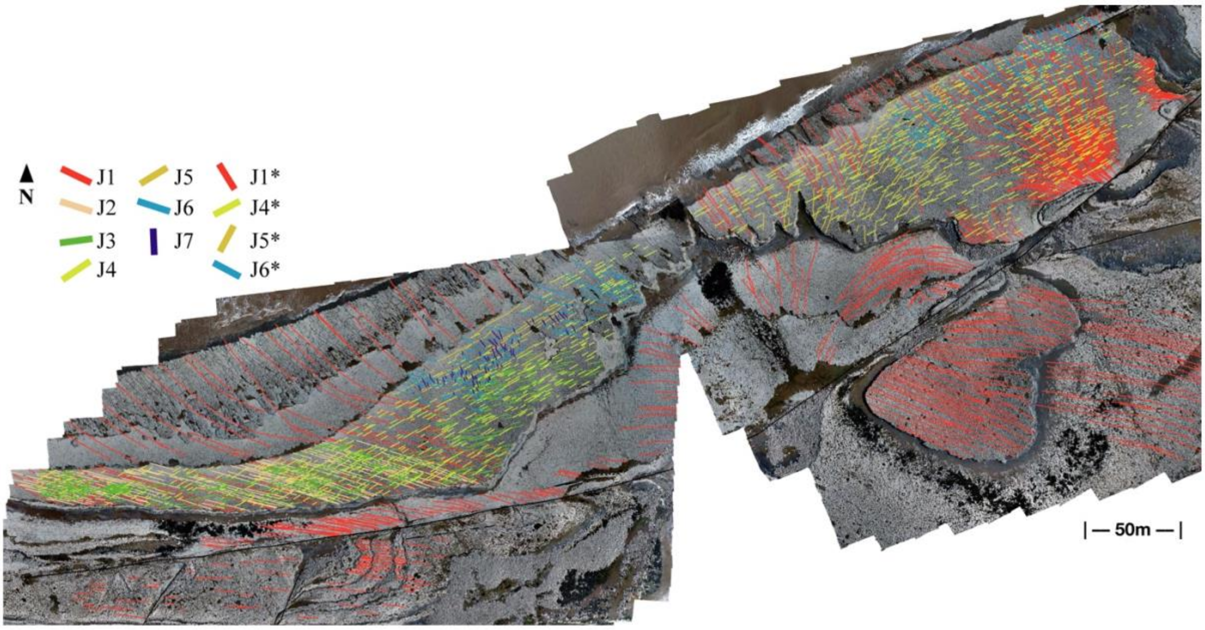


Fig. S1: Overview of the entire outcrop in a high detail image with all generations of mapped joints in Bench IV highlighted: for clarity, only part of the joints present are labelled. In adjacent limestone layers, only mapped joints of the oldest generations are shown.

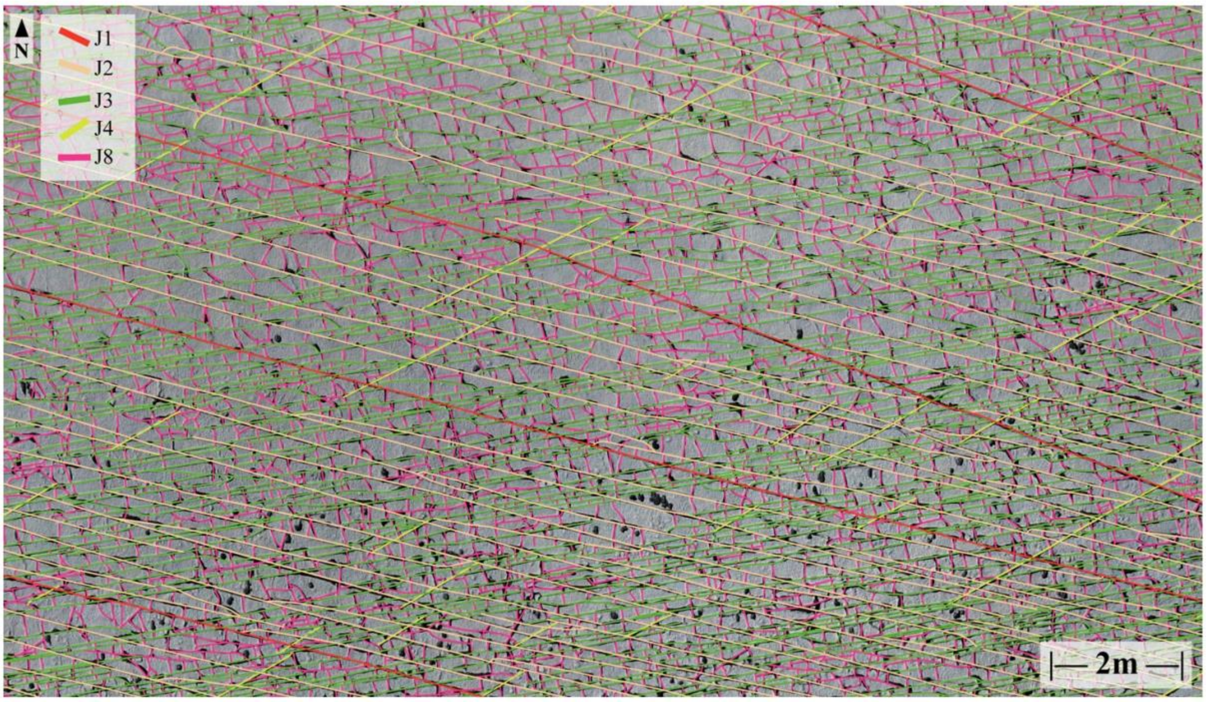


Fig. S2: High resolution image of a small part of Area W with all existing joints of all generations mapped, including J8. This is an enlargement of Figure 4F.